Pancreatic Disorders & Therapy
ISSN: 2165-7092

Hemsworth-Peterson, Pancreat Disord Ther 2013, 3:3
DOI: 10.4172/2165-7092.1000127

Research Article Open Access

Role of JNK Signalling and AHR in Fibrosis, Implications for New Therapeutics

Theresa C Hemsworth-Peterson*

Department of Medicine, Faculty of Medicine, Dalhousie University, Halifax, Canada

Abstract

In this study a role for signalling molecules in experimental fibrosis is established using a novel model of fibrosis. The yellow phosphorous treatment of AHR-/- knockout mice caused fibrosis within 7 days and provided a narrow window in which to characterize the regulation of signalling molecules. The mice used were AHR-/- mice (5 weeks) with and without Yellow Phosphorous (YP) treatment compared to C57BL/6 (5 weeks). YP (0.6 mg/kg) was administered to AHR-/- mice for 1 week. A subgroup of mice were also administered c-*jun* antisense. A group of AHR-/- mice (aged 10 to 24 week old) were also studied to verify the spontaneous development of liver fibrosis over time in these animals. As an index of fibrosis, the liver collagen content was determined by Sirius red/fast green staining in these animals, the levels of hepatic c-*Jun* and collagen were also assessed by Western analysis. Results indicate that without YP treatment, there was a significant spontaneous increase in the liver collagen content in the AHR-/- mice from weeks 5 to 24. Further, the results indicate that YP treatment increased the rate of fibrosis in AHR-/- mice and this increase in collagen content with only one week of YP treatment produced fibrosis (i.e., elevated collagen levels) equivalent to that seen in spontaneously in untreated 24 week old AHR-/- mice. Using Western analysis both c-*Jun* and collagen were found to be elevated in livers of 5 weeks old AHR-/- mice treated with YP. We thus identified an up regulation of c-jun and collagen indicating an increased rate of fibrosis in this new model. The use of c-jun antisense technology effectively reduced target molecules. In conclusion, molecular targets were identified in an accelerated model of hepatic fibrosis and using antisense technology the targets were inhibited and fibrosis was blocked.

Keywords: Fibrosis; Signalling molecules; Antisense technology

Introduction

Liver fibrosis has been defined as a disease in which excessive collagen is deposited in the liver leading to dysfunction of the liver. Hepatic stellate cells are the major liver cells involved in the development of liver fibrosis. They comprise about 15% of the total liver cells and are located in the sub endothelial space of Disse between the hepatocytes and the endothelial cells [1]. These cells are usually quiescent and they store lipid droplets. Upon activation by other factors they change into myofibroblast like cells and lose Vitamin A droplets and become proliferative, fibrogenic and contractile and act as major sources of extracellular matrix components [2]. HSC activation usually involves 2 steps i.e. initiation and perpetuation. HSC initiation is due to the stimuli released by the surrounding cells such as hepatocytes, endothelial cells, Kupffer cells, and platelets. The stimuli, which initiate these cells, are growth factors, inflammatory cytokines and reactive oxygen species or lipid peroxides [2]. As previously indicated, pancreatic fibrosis shows remarkable similarity to hepatic fibrosis [3].

Aryl Hydrocarbon Receptor (AHR) knockout mice were developed by the homologous recombination in the embryonic stem cells [4]. These mice have decreased ability to catabolize retinoic acid due to Ah receptor deficiency and this leads to liver fibrosis [5]. AHR knockout mice have genes coding for the Aryl hydrocarbon receptor protein deleted and the mice develop fibrosis at about 6-10 months of age [6]. Yellow phosphorous is a well-known toxic compound that produces degenerative changes characteristic of fibrosis and cirrhosis [7,8]. The animal model demonstrating these biochemical and histological changes characteristic of hepatic fibrosis was first established in our lab, liver fibrosis was induced in pigs by 8 weeks YP treatment (0.6 mg/kg) [8].

In the current study there was a significant increase in collagen content as the mice developed from week 5 to week 24 when they showed marked fibrosis, indicating that spontaneous fibrosis occurs in untreated AHR knockout mice over the 7 month time period. The results also indicate that one week of YP treatment increased the rate of fibrosis development in the AHR knockout mice such that fibrosis was evident in 5-week-old AHR knockout mice.

This increase in liver collagen content in 5 weeks old AHR knockout mice treated for one week with YP was equivalent to spontaneously elevated collagen levels in 24-week-old untreated AHR knockout mice. In this study the molecular changes occurring in this mouse model are investigated and antisense technology is used to intervene.

Methods

Animals and treatments

Mice (age 5 weeks) were treated with yellow phosphorous (0.6 mg/kg i.p.) for 1 week and compared to age matched controls. The mice were sacrificed and 15 μm sections of liver were stained by Sirius Red/Fast Green collagen staining technique to assess liver collagen content as an index of fibrosis. AHR knockout mice treated with yellow phosphorous were compared to untreated age matched AHR knockout mice and C57BL/6 mice controls (with and without treatment with yellow phosphorous). Collagen content was also assessed in AHR knockout mice aged 5-8 weeks, 10-12 weeks, 14-16 weeks and 24 weeks to demonstrate the spontaneous development of fibrosis in AHR knockout

***Corresponding author:** Theresa C Hemsworth-Peterson, Department of Medicine, Faculty of Medicine, Dalhousie University, Halifax, Canada, Tel: 902-494-2450; E-mail: terihemsworth@gmail.com

Received November 06, 2013; **Accepted** November 26, 2013; **Published** December 03, 2013

Citation: Hemsworth-Peterson TC (2013) Role of JNK Signalling and AHR in Fibrosis, Implications for New Therapeutics. Pancreat Disord Ther 3: 127. doi:10.4172/2165-7092.1000127

mice. In the experiments utilizing antisense, the phosphothioated c-*jun* antisense (5' GCAGTCATAGAACAGTCCGTCACTTCACGT-3' was administered (10 mg/kg) to a subgroup of AHR knockout mice, on three separate days via the tail vein, during the week of yellow phosphorous treatment.

Liver collagen estimation

The mice were sacrificed by injecting somnitol i.p. (0.05 ml). The liver was removed and 1cm x 1 cm piece of the liver was placed in 10% buffered formaldehyde and 4 % paraformaldehyde solution. The fixed liver tissue was embedded in paraffin and 5 (15 µm) sections were cut. The collagen content was evaluated by the Sirius Red/Fast Green staining [5]. The paraffin embedded 15 µm sections were deparaffinized by treatment with xylenes and ethanol. Then these tissue samples were incubated with Fast green FCF 0.04% (Gurr, BDH Chemicals, Canada) for 20 minutes and after subsequent washings they were again incubated with Fast green FCF 0.2% and Sirius Red F3B 0.08% (Gurr, BDH Chemicals, Canada) for 30 minutes and were then subsequently washed. Samples were eluted with 0.05N NaOH /50% methanol and were read in a spectrophotometer at 530 nm (Sirius red) and 605 nm (Fast Green). The average absorbance values were quantitated using their respective colour equivalencies [6,9] i.e. 38.4 for Sirius red and 2.08 for Fast green. The non-collagenous protein (mg) was determined as absorbance 605nm/2.08 and the collagen (µg) protein was calculated as absorbance 530 nm- 0.26 absorbance 605 nm/38.4. Finally the collagen content (µg/mg total protein) was determined as µg collagen/ µg collagen + mg non –collagenous protein [6].

Western analysis

Liver tissue lysates were prepared by pulverizing frozen tissue with a liquid nitrogen-cooled mortar and pestle. Ice-cold RIPA buffer (1% Igepal CA 630, 0.5% sodium deoxycholate, 0.1% SDS in PBS, pH 7.4) containing standard protease inhibitors (PMSF, aprotinin, sodium orthovanadate) was added at a ratio of 3uL RIPA/mg tissue. Suspensions were homogenized followed by sonication and were incubated on ice for 30 minutes with additional PMSF (0.03 uL/mg tissue) before centrifugation (10 min, 10,000 rpm, 4°C). Supernatants (lysates) were stored at -86°C. Protein estimation was done using the QuantiPro BCA Assay Kit (Sigma-Aldrich). 50 µg of protein were run on 10% Tris-HCl gels (Bio-Rad) and transferred to PVDF membranes overnight. Proteins were probed with primary antibody, e.g., c-*Jun* (1:1000; New England Biolabs); secondary antibody (Anti-rabbit; 1:2000) was applied and protein bands were visualized with LumiGlo (New England Biolabs). Densitometry was done using Scion Image software. Results are expressed as Relative Density Units (RDU).

Statistical analysis

An unpaired Student's t-test was used to compare two variables and an analysis of variance Student-Newman-Keul's test was used while comparing more than two variables [10].

Results

Collagen content in untreated AHR knockout mice over 24 weeks

The collagen content in liver sections taken from AHR knockout mice (AHR-/-) of various ages is shown in Figure 1. Collagen content was determined in liver sections of AHR knockout mice (5-8 weeks) and compared with other age groups and was expressed as µg/mg protein. There was a significant increase (*p<0.001, when compared to 5-8 weeks) in collagen content as the mice developed, which indicated

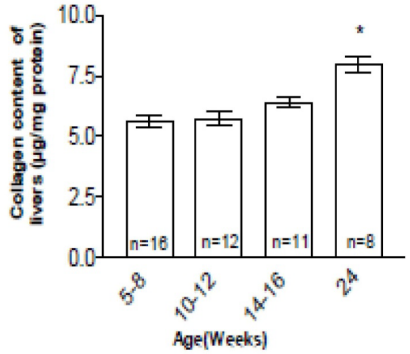

Figure 1: Quantitation of collagen content in liver sections taken from AHR knockout mice (AHR -/-) mice of various ages. Collagen content is shown in liver sections of AHR knockout mice (5-8 weeks) and compared to other age groups and is expressed as µg/mg protein. *p<0.001, significantly elevated when compared to 5-8 weeks.

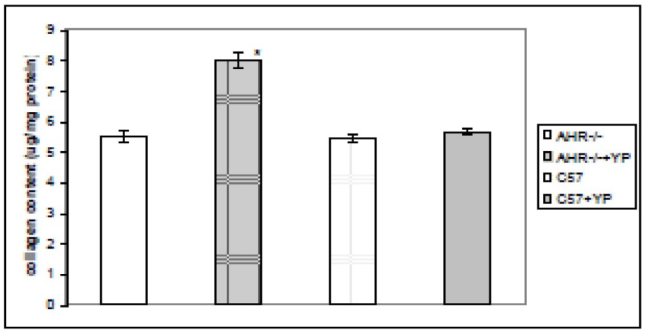

Figure 2: Collagen content in livers of C57BL/6 mice with and without treatment with YP for 1 week in contrast to the effect of Yellow phosphorous (1 wk) on the development of liver fibrosis in AHR knockout mice (AHR -/-). *p<0.001, significantly different from corresponding age-matched controls.

that fibrosis developed spontaneously in AHR knockout mice between 5 weeks and 24 weeks of age.

Collagen content in AHR knockout mice treated with yellow phosphorous

Liver collagen content was determined in 5 week old AHR-/- mice with and without treatment with YP and contrasted to the collagen content in C57BL/6 mice with and without YP treatment. There was no significant difference in collagen content (ug/mg protein) in livers of C57BL/6 mice with and without treatment for 1 week with YP (Figure 2). In contrast, following 1 week of YP treatment in AHR knockout mice, there was a significant increase ($p<0.001$) in collagen content compared to age matched controls, representing a 46% increase in the collagen content when compared to untreated AHR knockout mice. This increase in collagen content following YP (1 week) treatment in 5 week old AHR knockout mice was equivalent to collagen levels in untreated 24 week old AHR knockout mice.

Effect of yellow phosphorous treatment of c-*Jun* in AHR knockout mice

Treatment of the AHR-/- mice with yellow phosphorous for only 4 days significantly increased c-*Jun* two fold compared to untreated AHR-/- mice (Figure 3). Based on these results we determined the optimum time to treat mice with c-*jun* antisense in subsequent experiments.

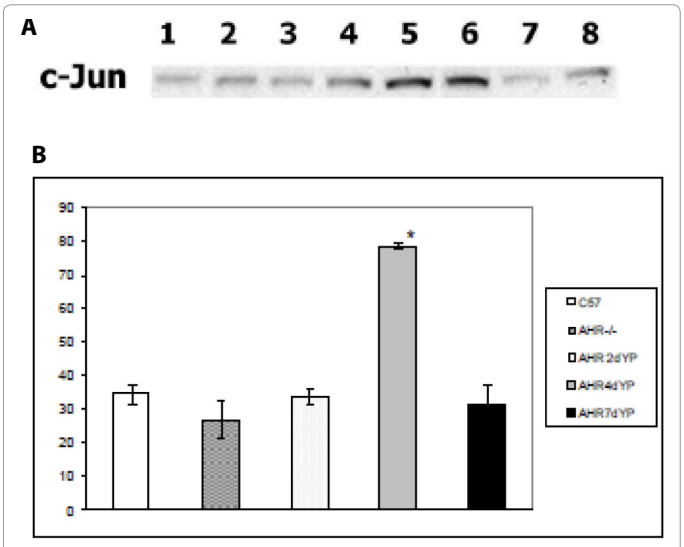

Figure 3: Effect of YP treatment on c-*Jun* in livers of AHR-/- mice at several time points after treatment. A representative Western (Panel A) showing the effect of YP treatment on c-*Jun* in livers of AHR-/- mice compared to control. The liver lysates samples were C57 (lane 1), AHR-/- (lane 2), AHR-/- treated for 2 days with YP (lanes 3 and 4), AHR-/- treated for 4 days with YP (lanes 5 and 6), AHR-/- treated for 7 days with YP (lanes 7 and 8). Equal protein loading on lanes was verified by anti- β actin antibody. *p<0.05, significantly different compared to control and other groups.

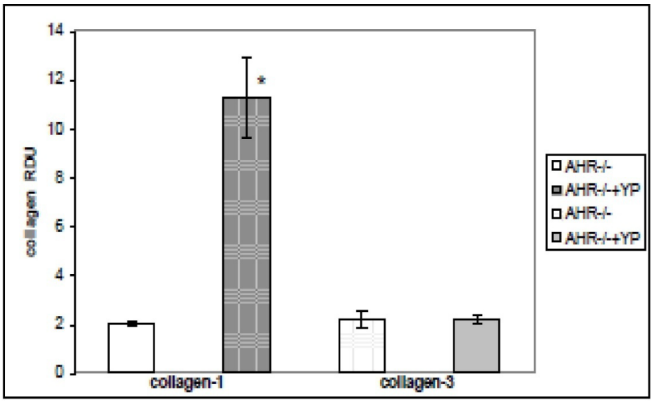

Figure 4: Collagen -1 and collagen-3 in livers of YP treated AHR-/- mice compared to untreated AHR/- mice. *p<0.05, significantly different compared to untreated AHR-/- mice.

Effect of yellow phosphorous treatment on collagen -1 in AHR knockout mice

The results shown in Figure 4 indicate that treatment of the AHR-/- mice with yellow phosphorous for 2 weeks significantly elevated collagen type 1 compared to untreated AHR-/- mice. It is interesting to note that no change was observed in collagen type 3 in AHR-/- mice treated with yellow phosphorous for 2 weeks.

Demonstration of c-*jun* fluorescence in liver sections following tail vein injection

Following injection of c-*jun* antisense via the tail vein, the c-*jun* antisense effectively reached the liver, shown as positive fluorescein labelled c-*jun* antisense by fluorescence microscopy of the liver (Figure 5).

Effect of c-jun antisense on c-*Jun* and collagen -1 in liver of AHR knockout mice

The results shown in Figure 6 illustrate the effect of c-*jun* antisense on c-*jun* (Figure 6A) and coll-1 (Figure 6B) in the AHR-/- mice which had also been treated with yellow phosphorous. The c-*jun* antisense significantly reduced the c-*Jun* and coll-1 in livers of AHR-/- mice treated with yellow phosphorous; this is in contrast to the lack of effect that occurred using missense.

Discussion

Liver fibrosis is characterized by a significant elevation in hepatic collagen content. Sirius red/Fast green staining allows us to quantitate

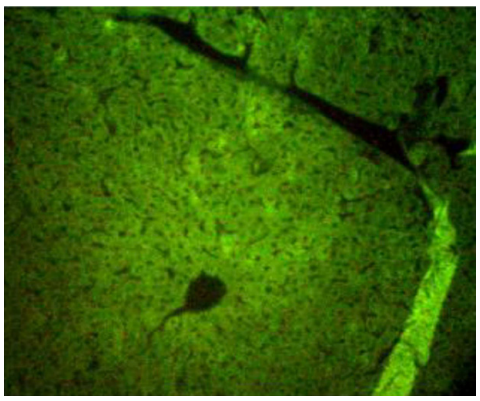

Figure 5: Fluorescence microscopy of the liver following injection of fluorescein labelled c-jun antisense via the tail vein.

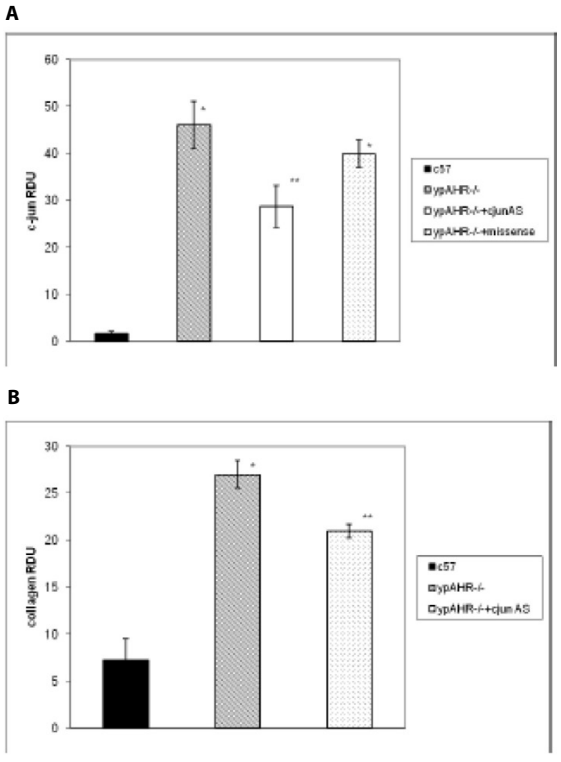

Figure 6: The effect of c-*jun* antisense on c-Jun (Figure 6A) and coll-1 (Figure 6B) in the AHR-/- mice which had also been treated with yellow phosphorous. *p<0.05, significantly different compared to control C57 mice. **p<0.05 compared to YP treated AHR-/- mice.

the collagen deposition in liver sections [6,8,9]. Our results established that there was a significant spontaneous increase in the liver collagen content as the AHR knockout mice developed from 5 weeks to 24 weeks of age. The results also indicate that one week of YP treatment increased hepatic fibrosis in 5-week-old AHR-/- mice and this increase in liver collagen content was equivalent to spontaneously elevated collagen levels in fibrotic 24 week old AHR-/- mice. This is in contrast to C57BL/6 mice where the hepatic collagen content was not changed following one week treatment with YP. Hence the knockout of the AHR results in hepatic fibrosis which can be accelerated with the addition of another known fibrogenic agent, in this case, yellow phosphorous. Interestingly, a recent report indicates the protective role of AHR in acute pancreatitis induced by cerulein and further suggests this occurs through regulation of pancreatic IL-22 [11]. The AHR knockout mouse will spontaneously develop hepatic fibrosis and eventually develops hepatocellular carcinoma. In a similar fashion, it is well established that chronic pancreatitis can contribute to pancreatic cancer which is characterized by an extensive collagen deposition i.e., fibrosis [12].

The yellow phosphorous treatment of AHR-/- mice represents a novel way to accelerate liver fibrosis in an animal model and such a model may prove useful in other forms of fibrosis including pancreatic fibrosis. This fibrosis model is more rapid than the AHR-/- model or YP model alone. We characterized several key molecular changes in this YP induced liver fibrosis model in AHR-/- mice with Western analysis and our results indicate that c-*jun* and collagen type -1 are elevated. Using this information we intervened with c-*jun* antisense technology. In contrast to a lack of effect of missense, the c-*jun* antisense significantly reduced the c-*jun* and coll-1 in livers of AHR-/-mice treated with yellow phosphorous.

We have previously shown that the drug pentoxifylline (PTX) [13] blocks fibro proliferation and collagen synthesis by inhibiting phosphorylation of c-*jun* and thus blocks c-*jun* mediated signalling including signalling via the PDGF receptor. PTX also prevents both the biochemical and histological changes associated with hepatic fibrosis in the animal model of liver disease [8,14]; PTX inhibits neutrophil function [15-17], which may be important since neutrophils play a major role in mediating inflammatory conditions [18-20] and PTX prevents the fibro proliferative effect of PDGF in vitro [21-25]. PTX will reduce fibrosis in cirrhotic patients who undergo resections and decrease collagen deposition in colitis [26,27] and prevent fibrosis in an animal model [23,28,29]. PTX can also reduce fibro proliferation in early stages of injury in the bile duct ligated rat model [28] and down regulate c-*jun* gene expression known to be involved in growth and proliferation of fibrogenic cells [13,30]. Our studies indicated that PTX alters hepatic stellate cell function and other fibrotic parameters [31]. A recent report suggests that PTX modulates oxidative and nitrosative stress in acute pancreatitis [32], further suggesting the potential therapeutic role for PTX in acute pancreatitis.

The activation of c-*jun* is important in the up regulated expression of growth and proliferation genes [33] and phosphorylated-c-*jun* is known to stimulate expression of proliferative genes that promote HSC proliferation during liver fibrosis [13,34]. PTX, normally used to treat vascular disorders [35], decreases fibroblast [36,37] and HSC proliferation [38], decreases PDGF stimulated fibro proliferation and collagen synthesis [23,39] and inhibits IL-18 production [40], NFκB activation [41] and can also down regulate the expression of c-*jun* in HSCs [13]. HSCs are activated in liver fibrosis [2,42] and express α-smooth muscle actin (α-SMA) [43,44]. We have reported that sera obtained fibrotic HCV patients stimulated HSC proliferation and phosphorylation of c-j*un* on ser 73, which was decreased by PTX [45]. Recent results suggest that PTX can protect mitochondria in cerulein induced pancreatitis [46].

In this study the technique of Neurath et al. [47] was used to deliver antisense.

Our initial studies using the c-*jun* antisense involved dose-finding and duration-finding experiments. Our data indicates that we can visualize the c-*jun* antisense in the liver. Tail vein administration of c-*jun* antisense downregulated c-*jun* expression in the livers and this was verified using immunoblots to verify a decrease in c-*jun* protein levels in livers.

These studies were done in the accelerated model of fibrosis that was developed by administering yellow phosphorous to the AHR-/- mouse. A role for signalling molecules in experimental fibrosis was established using this novel accelerated model of fibrosis which we developed. The yellow phosphorous treatment of AHR-/- knockout mice caused fibrosis within 7 days and provided a narrow window in which to characterize the up regulation of signalling molecules and in this study an up regulation of c-*jun* was documented. The accelerated model allowed the identification of targets and also provided a reasonable treatment period to inhibit these target molecules. These results together with this accelerated fibrosis model may have significant application in pancreatic fibrosis where there appears to be significant overlap in target cells, mechanism and cytokine involvement [4]. Very recently, a report suggests that JNK signaling may play a significant role in production of reactive oxygen species in cerulein-induced acute pancreatitis [48].

In summary, this study characterized the early stimulation of c-*jun* and collagen type 1 in the accelerated fibrotic mouse model and employed antisense technology to block the increase in c-*Jun* and prevent the subsequent increase in collagen, thus blocking fibrosis. These findings could play a significant role in understanding the underlying mechanism in pancreatic fibrosis and have implications in the development of new therapeutics for the treatment of both hepatic and pancreatic fibrosis.

Acknowledgments

This project was supported by a grant from Canadian Institute of Health Research.

References

1. Kaplowitz N (1992) Liver and biliary diseases. Williams & Wilkins Baltimore, USA.
2. Hui AY, Friedman SL (2003) Molecular basis of hepatic fibrosis. Expert Rev Mol Med 5: 1-23.
3. Hemsworth-Peterson TC (2012) Pancreatic and Hepatic Fibrosis: Remarkable Similarities. Pancreatic Dis Ther 2: e111.
4. Fernandez-Salguero P, Pineau T, Hilbert DM, McPhail T, Lee SS, et al. (1995) Immune system impairment and hepatic fibrosis in mice lacking the dioxin-binding Ah receptor. Science 268: 722-726.
5. Andreola F, Fernandez-Salguero PM, Chiantore MV, Petkovich MP, Gonzalez FJ, et al. (1997) Aryl hydrocarbon receptor knockout mice (AHR-/-) exhibit liver retinoid accumulation and reduced retinoic acid metabolism. Cancer Res 57: 2835-2838.
6. Peterson TC, Hodgson P, Fernandez-Salguero P, Neumeister M, Gonzalez FJ (2000) Hepatic fibrosis and cytochrome P450: experimental models of fibrosis compared to AHR knockout mice. Hepatol Res 17: 112-125.
7. Mallory FB (1933) Phosphorus and Alcoholic Cirrhosis. Am J Pathol 9: 557-568.
8. Peterson TC (1993) Pentoxifylline prevents fibrosis in an animal model and inhibits platelet-derived growth factor-driven proliferation of fibroblasts. Hepatology 17: 486-493.

9. López-De León A, Rojkind M (1985) A simple micromethod for collagen and total protein determination in formalin-fixed paraffin-embedded sections. J Histochem Cytochem 33: 737-743.

10. Zar JH (1974) Biostatistical methods. Englewood Cliffs, NewJersy Prentice Hall USA.

11. Xue J, Nguyen DT, Habtezion A (2012) Aryl hydrocarbon receptor regulates pancreatic IL-22 production and protects mice from acute pancreatitis. Gastroenterology 143: 1670-1680.

12. Shields MA, Ebine K, Sahai V, Kumar K, Siddiqui K, et al. (2013) Snail cooperates with KrasG12D to promote pancreatic fibrosis. Mol Cancer Res 11: 1078-1087.

13. Peterson TC, Peterson MR, Robertson HA, During M, Dragunow M (2002) Selective down-regulation of c-jun gene expression by pentoxifylline and c-jun antisense interrupts platelet-derived growth factor signaling: pentoxifylline inhibits phosphorylation of c-Jun on serine 73. Mol Pharmacol 61: 1476-1488.

14. Isbrucker RA, Peterson TC (1994) Collagens a (I) and a (III) mRNA levels are increased in a porcine model of hepatic fibrosis and reduced by PTX administration. Gastroenterol 106: 1086.

15. Crowley JJ, Waldman SA, Raffin TA (1990) Attenuation of neutrophil mediated acute lung injury. The Pulmonary Circulation and Acute Lung Injury. Said SI, Futura Publishing New York, USA.

16. Ishizaka A, Wu ZH, Stephens KE, Harada H, Hogue RS, et al. (1988) Attenuation of acute lung injury in septic guinea pigs by pentoxifylline. The American review of respiratory disease 138: 376-382.

17. Mandell GL (1988) ARDS, neutrophils, and pentoxifylline. Am Rev Respir Dis 138: 1103-1105.

18. Lilly CM, Sandhu JS, Ishizaka A, Harada H, Yonemaru M, et al. (1989) Pentoxifylline prevents tumor necrosis factor-induced lung injury. Am Rev Respir Dis 139: 1361-1368.

19. Raffin TA (1990) Acute lung injury and pentoxifylline. Crit Care Med 18: 1485-1486.

20. Senior RM, Huang JS, Griffin GL, Deuel TF (1985) Dissociation of the chemotactic and mitogenic activities of platelet-derived growth factor by human neutrophil elastase. J Cell Biol 100: 351-356.

21. Peterson TC, Neumeister M (1996) Effect of pentoxifylline in rat and swine models of hepatic fibrosis: role of fibroproliferation in its mechanism. Immunopharmacology 31: 183-193.

22. Peterson TC, Isbrucker RA, Hooper ML (1994) In vitro effect of platelet-derived growth factor on fibroproliferation and effect of cytokine antagonists. Immunopharmacology 28: 259-270.

23. Isbrucker RA, Peterson TC (1998) Platelet-derived growth factor and pentoxifylline modulation of collagen synthesis in myofibroblasts. Toxicol Appl Pharmacol 149: 120-126.

24. Peterson TC, Isbrucker RA (1992) Fibroproliferation in liver disease: role of monocyte factors. Hepatology 15: 191-197.

25. Peterson TC, Huet PM (1997) PTX but not UDCA or TUDCA inhibit the proliferative effect of sera samples from PBC patients. Hepatol Res 7: 94-104.

26. Peterson TC, Tanton RT (1996) Effect of PTX in Collagenous Colitis; a new therapy? Gastroenterology.

27. Peterson TC, Davey K (1997) Effect of acute pentoxifylline treatment in an experimental model of colitis. Aliment Pharmacol Ther 11: 575-580.

28. Dagenais M, Rocheleau B, Giroux L, Huet PM, Pomier-Layrargues G (1990) Pentoxiphylline as a medical treatment for portal hypertension in cirrhotic rats. Gastroenterology 98: A580.

29. Peterson TC, Wornell P, Peterson M, Dragunow M (1999) Characterization of mouse model of yellow phosphorous induced hepatic fibrosis. Hepatology 30: 542A.

30. Ji Q, Zhang L, Jia H, Xu J (2004) Pentoxifylline inhibits endotoxin-induced NF-kappa B activation and associated production of proinflammatory cytokines. Ann Clin Lab Sci 34: 427-436.

31. Verma-Gandhu M, Peterson MR, Peterson TC (2007) Effect of fetuin, a TGFbeta antagonist and pentoxifylline, a cytokine antagonist on hepatic stellate cell function and fibrotic parameters in fibrosis. Eur J Pharmacol 572: 220-227.

32. Escobar J, Pereda J, Arduini A, Sandoval J, Moreno ML, et al. (2012) Oxidative and nitrosative stress in acute pancreatitis. Modulation by pentoxifylline and oxypurinol. Biochem Pharmacol 83: 122-130.

33. Angel P, Karin M (1991) The role of Jun, Fos and the AP-1 complex in cell-proliferation and transformation. Biochim Biophys Acta 1072: 129-157.

34. Mann DA, Smart DE (2002) Transcriptional regulation of hepatic stellate cell activation. Gut 50: 891-896.

35. Ward A, Clissold SP (1987) Pentoxifylline. A review of its pharmacodynamic and pharmacokinetic properties, and its therapeutic efficacy. Drugs 34: 50-97.

36. Strutz F, Heeg M, Kochsiek T, Siemers G, Zeisberg M, et al. (2000) Effects of pentoxifylline, pentifylline and gamma-interferon on proliferation, differentiation, and matrix synthesis of human renal fibroblasts. Nephrol Dial Transplant 15: 1535-1546.

37. Berman B, Duncan MR (1989) Pentoxifylline Inhibits Normal Human Dermal Fibroblast In Vitro Proliferation, Collagen, Glycosaminoglycan, and Fibronectin Production, and Increases Collagenase Activity. J Invest Dermatol 92: 605-610.

38. Isbrucker RA, Peterson TC (1995) Effect of PDGF, PTX and metabolite-1 on collagen production in orcine HSCs. Hepatol 22.

39. Peterson TC (1996) Inhibition of fibroproliferation by pentoxifylline. Activity of metabolite-1 and lack of role of adenosine receptors. Biochem Pharmacol 52: 597-602.

40. Samardzic T, Jankovic V, Stosic-Grujicic S, Popadic D, Trajkovic V (2001) Pentoxifylline inhibits the synthesis and IFN-gamma-inducing activity of IL-18. Clin Exp Immunol 124: 274-281.

41. Ji Q, Zhang L, Jia H, Xu J (2004) Pentoxifylline inhibits endotoxin-induced NF-kappa B activation and associated production of proinflammatory cytokines. Ann Clin Lab Sci 34: 427-436.

42. Svegliati-Baroni G, Saccomanno S, van Goor H, Jansen P, Benedetti A, et al. (2001) Involvement of reactive oxygen species and nitric oxide radicals in activation and proliferation of rat hepatic stellate cells. Liver 21: 1-12.

43. Cheng J, Imanishi H, Liu W, Iwasaki A, Ueki N, et al. (2002) Inhibition of the expression of alpha-smooth muscle actin in human hepatic stellate cell line, LI90, by a selective cyclooxygenase 2 inhibitor, NS-398. Biochem Biophys Res Commun 297: 1128-1134.

44. Buniatian GH (2003) Stages of activation of hepatic stellate cells: effects of ellagic acid, an inhibiter of liver fibrosis, on their differentiation in culture. Cell Prolif 36: 307-319.

45. Khan F, Peltekian KM, Peterson TC (2008) Effect of interferon-alpha, ribavirin, pentoxifylline, and interleukin-18 antibody on hepatitis C sera-stimulated hepatic stellate cell proliferation. J Interferon Cytokine Res 28: 643-651.

46. Gómez-Cambronero L, Camps B, de La Asunción JG, Cerdá M, Pellín A, et al. (2000) Pentoxifylline ameliorates cerulein-induced pancreatitis in rats: role of glutathione and nitric oxide. J Pharmacol Exp Ther 293: 670-676.

47. Neurath MF, Pettersson S, Büschenfelde KHMZ, Strober W (1996) Local administration of antisense phosphorothiate olignucleotides to the p65 subunit of NF−kappaB abrogates established experimental colitis in mice. Nat Med 2: 998-1004.

48. Sledzinski M, Borkowska A, Sielicka-Dudzin A, Halon M, Wozniak M, et al. (2013) Cerulein-induced acute pancreatitis is associated with c-Jun NH(2)-terminal kinase 1-dependent ferritin degradation and iron-dependent free radicals formation. Pancreas 42: 1070-1077.